

This is a copy of the published version, or version of record, available on the publisher's website. This version does not track changes, errata, or withdrawals on the publisher's site.

MOONS – Multi Object spectroscopy for the VLT: overview and instrument integration update

Oscar Gonzalez, Michele Cirasuolo, William Taylor, Martin Black, Philip Rees, et al.

Published version information:

Citation: O Gonzalez et al. MOONS – multi object spectroscopy for the VLT: overview and instrument integration update. Proc SPIE 12184 (2022): 1218412. Is in proceedings of: Conference on Ground-Based and Airborne Instrumentation for Astronomy IX, Montreal, CANADA, 17-22 Jul 2022

DOI: [10.1117/12.2629932](https://doi.org/10.1117/12.2629932)

Copyright 2022 Society of Photo-Optical Instrumentation Engineers (SPIE). One print or electronic copy may be made for personal use only. Systematic reproduction and distribution, duplication of any material in this publication for a fee or for commercial purposes, and modification of the contents of the publication are prohibited.

This version is made available in accordance with publisher policies. Please cite only the published version using the reference above. This is the citation assigned by the publisher at the time of issuing the APV. Please check the publisher's website for any updates.

This item was retrieved from **ePubs**, the Open Access archive of the Science and Technology Facilities Council, UK. Please contact epublications@stfc.ac.uk or go to <http://epubs.stfc.ac.uk/> for further information and policies.

PROCEEDINGS OF SPIE

[SPIDigitalLibrary.org/conference-proceedings-of-spie](https://spiedigitallibrary.org/conference-proceedings-of-spie)

MOONS – multi object spectroscopy for the VLT: overview and instrument integration update

Oscar Gonzalez, Michele Cirasuolo, William Taylor, Martin Black, Philip Rees, et al.

Oscar Gonzalez, Michele Cirasuolo, William Taylor, Martin Black, Philip Rees, Ian Bryson, Stephen Chittick, Jose Afonso, Simon Lilly, Hector Flores, Roberto Maiolino, Ernesto Oliva, Stephane Paltani, Leonardo Vanzi, Manuel Abreu, Jean-Philippe Amans, David Atkinson, Steven Beard, Andrea Belfiore, Ciaran Breen, Amelia Bayo, Andy Born, Alexandre Cabral, Lee Chapman, William Cochrane, João Coelho, Miriam Colling, Ralf Conzelmann, Francesco Dalessio, George Davidson, Françoise Delplancke-Ströbele, Martin Fisher, Vincenzo Forchi, Paolo Franzetti, Bianca Garilli, Adriana Gargiulo, Isabelle Guinouard, Pablo Gutierrez, Régis Haigron, Peter Hammersley, Valentin Ivanov, Derek Ives, Olaf Iwert, David King, Suzanne Kovacz, Philippe Laporte, David Lee, Gianluca Li Causi, Alastair Macleod, Domingo Alvarez Mendez, António Oliveira, Ralf Palsa, Manuel Parra, Fernando Pedichini, Vicente Peña, Monika Petr-Gotzens, Myriam Rodrigues, Frédéric Royer, Pedro Santos, Jorge Sepulveda, Robyn Sharman, Tzu-Chiang Shen, Michael Sordet, Jonathan Strachan, Graham Tait, Alexis Tejada, Andrea Tozzi, Norman O'Malley, Chris Waring, Stephen Watson, Bart Willemse, Xiaofeng Gao, Yanbin Yang, Manuela Zoccali, "MOONS – multi object spectroscopy for the VLT: overview and instrument integration update," Proc. SPIE 12184, Ground-based and Airborne Instrumentation for Astronomy IX, 1218412 (29 August 2022); doi: 10.1117/12.2629932

SPIE.

Event: SPIE Astronomical Telescopes + Instrumentation, 2022, Montréal, Québec, Canada

MOONS – Multi Object spectroscopy for the VLT: overview and instrument integration update

Oscar A. Gonzalez^{*a}, Michele Cirasuolo^b, William Taylor^a, Martin Black^a, Phil Rees^a, Ian Bryson^a, Stephen Chittick^a, Jose Afonso^{c,d}, Simon Lilly^c, Hector Flores^f, Roberto Maiolino^g, Ernesto Oliva^h, Stephane Paltaniⁱ, Leonardo Vanzij, Manuel Abreu^{c,d}, Jean-Philippe Amans^f, David Atkinson^a, Steven Beard^a, Andrea Belfiore^m, Ciaran Breen^a, Amelia Bayo^b, Andy Born^a, Alexandre Cabral^{c,d}, Lee Chapman^a, William Cochrane^a, João Coelho^{c,d}, Miriam Colling^k, Ralf Conzelmann^b, Francesco Dalessio^l, George Davidson^a, Françoise Delplancke-Ströbele^b, Martin Fisher^g, Vincenzo Forchi^b, Paolo Franzetti^m, Bianca Garilli^m, Adriana Gargiulo^m, Isabelle Guinouard^f, Pablo Gutierrez^b, Régis Haigron^f, Peter Hammersley^b, Valentin Ivanov^b, Derek Ives^b, Olaf Iwert^b, David Kingⁿ, Suzanne Kovacz^b, Philippe Laporte^f, David Lee^a, Gianluca Li Causi^l, Alastair Macleod^a, Domingo Alvarez^b, António Oliveira^{c,d}, Ralf Palsa^b, Manuel Parra^o, Fernando Pedichini^l, Vicente Peña^o, Monika Petr-Gotzens^b, Myriam Rodrigues^f, Frédéric Royer^f, Pedro Santos^{c,d}, Jorge Sepulveda^o, Robyn Sharman^a, Tzu-Chiang Shen^o, Michael Sordetⁱ, Jonathan Strachan^a, Graham Tait^a, Alexis Tejada^o, Andrea Tozzi^h, Norman O'Malley^a, Chris Waring^a, Stephen Watson^a, Bart Willemse^a, Gao Xiaofeng^a, Yanbin Yang^f, Manuela Zoccali^j

^a STFC, UK Astronomy Technology Centre, Royal Observatory Edinburgh, Edinburgh, EH9 3HJ, UK; ^b ESO, Karl-Schwarzschild-Str. 2, 85748, Garching bei München, Germany; ^c Instituto de Astrofísica e Ciências do Espaço, Universidade de Lisboa, Campus do Lumiar, Estrada do Paço do Lumiar 22, Edif. D, PT1649-038 Lisboa, Portugal; ^d Laboratório de Óptica, Lasers e Sistemas, Departamento de Física, Faculdade de Ciências, Universidade de Lisboa, Campo Grande 1749-016 Lisboa, Portugal; ^e ETH Zurich, Department of Physics, Wolfgang-Pauli-Strasse 27, 8093 Zurich, Switzerland; ^f GEPI, CNRS, Observatoire de Paris, PSL University, France; ^g Department of Physics, Cavendish Laboratory, JJ Thomson Avenue, Cambridge, CB3 0HE, UK; ^h INAF-Osservatorio Astrofisico di Arcetri, Largo Enrico Fermi 5, I – 50125, Florence, Italy; ⁱ Department of Astronomy, University of Geneva, ch. d'Écogia 16, CH-1290 Versoix, Switzerland; ^j Pontificia Universidad Católica de Chile, Av. Vicuña Mackenna 4860, 7820436 Macul, Santiago, Chile; ^k STFC, Rutherford Appleton Laboratory, Harwell Campus, Oxfordshire, OX11 0QX, UK; ^l INAF-Osservatorio Astronomico di Roma, Viale del Parco Mellini 84, Roma, Italy; ^m INAF - IASF Milano, Via E. Bassini 15, I-20133 Milano, Italy; ⁿ Institute of Astronomy, University of Cambridge, Madingley Road, Cambridge, CB3 0HA, UK; ^o BlueShadows Ltda., Barros Errazurriz, 1954, OF 706, Santiago, Chile

ABSTRACT

The Multi Object Optical and Near-infrared Spectrograph (MOONS) instrument is the next generation multi-object spectrograph for the Very Large Telescope (VLT). The instrument combines the high multiplexing capability offered by 1000 optical fibres deployed by individual robotic positioners with a novel spectrograph able to provide both low- and high-resolution spectroscopy simultaneously across the wavelength range 0.64 μ m - 1.8 μ m. Powered by the collecting area of the 8-m VLT, MOONS will provide the astronomical community with a world-leading facility able to serve a wide range of Galactic, Extragalactic and Cosmological studies. This paper provides an updated overview of the instrument and its construction progress, reporting on the ongoing integration phase.

Keywords: Multi-object Spectrograph, Optical and near-IR spectrograph, medium and high-resolution spectrograph

* oscar.gonzalez@stfc.ac.uk; +44 131 668 8267; www.stfc.ukri.org

1. INTRODUCTION

Over the last two decades several key observational efforts have dramatically changed our knowledge of the Universe. Yet, some of the most fundamental problems in science remain to be solved: understanding the nature of the dark components which dominate the global expansion and Large-Scale Structure of the Universe and the physical processes that affect baryons and shape the formation and evolution of stars and galaxies. Answering these questions demands an accurate reconstruction of the assembly history of stars and galaxies over virtually all cosmic times to decode the building blocks of the Universe.

The Milky Way offers a one-of-a-kind opportunity to reconstruct the assembly history of a prototypical spiral galaxy by looking at the individual chemical abundances, ages, and orbital movements of its stellar populations down to its innermost components. On the other hand, tracing the evolution of galaxy properties beyond our own galaxy (star-formation, metallicity, mass-assembly, etc.), over the whole cosmic epoch, is key to understand the effects of age and environment. In fact, pushing these studies to the highest redshifts - when the Universe was just a few hundred million years old - provides the opportunity to investigate the physics of the early Universe and cosmic re-ionization. These ambitious science goals require an accurate determination of stellar and galactic physical properties for as many stars and galaxies as possible.

To this end, the MOONS instrument has been developed focusing on three essential requirements: sensitivity, multiplex and wavelength coverage. The high sensitivity is being achieved by optimising all the components of the MOONS instrument for high transmission that is coupled with the large aperture and efficiency of the VLT. The multiplex of 1000 is a factor 20 more than current spectrographs operating in the near-infrared, thus pushing the limit on budget, technical capability to manufacture the very large optics, as well as the mass and volume available at the Nasmyth platform for the large MOONS cryostat.

Finally, the broad wavelength coverage of MOONS of $0.645\mu\text{m} - 1.8\mu\text{m}$, extending in the near-IR is critical to observe heavily dust-obscured regions of our Milky Way as well to open the window onto the high-redshift Universe. To meet the aspirations of both the Galactic and Extragalactic scientific communities, MOONS offers both low- and high-resolution spectroscopy. In the low-resolution mode ($R\sim 4,000-6,000$), the entire $0.645-1.8\mu\text{m}$ range is observed simultaneously, across the RI, YJ and H atmospheric windows. In the high-resolution mode three carefully selected windows are simultaneously covered: the YJ channel that remains at $R\sim 4000$, an RI channel with $R>9,000$ around the CaT region to measure stellar radial velocities, and another with $R\sim 19,000$ in the H-bands for detailed measurements of chemical abundances. Details on the instrument specifications can be found at www.vltmoons.org.

2. INSTRUMENT DESCRIPTION

2.1 MOONS technical overview

The instrument will be installed at the Nasmyth A of UT1 of the VLT. MOONS comprises two main sections, the Rotating Front End (RFE) and the Triple Arm Spectrograph (TAS). A labelled image of the two sections illustration is shown in Figure 1, which highlights different aspects of the instrument. These are briefly described in the subsequent subsections together with an update on their integration procedure. A detailed description of all MOONS components can be found in [1] and in dedicated papers for the different subsystems [2], [3], [4], [5], [6], [7], [8], [9].

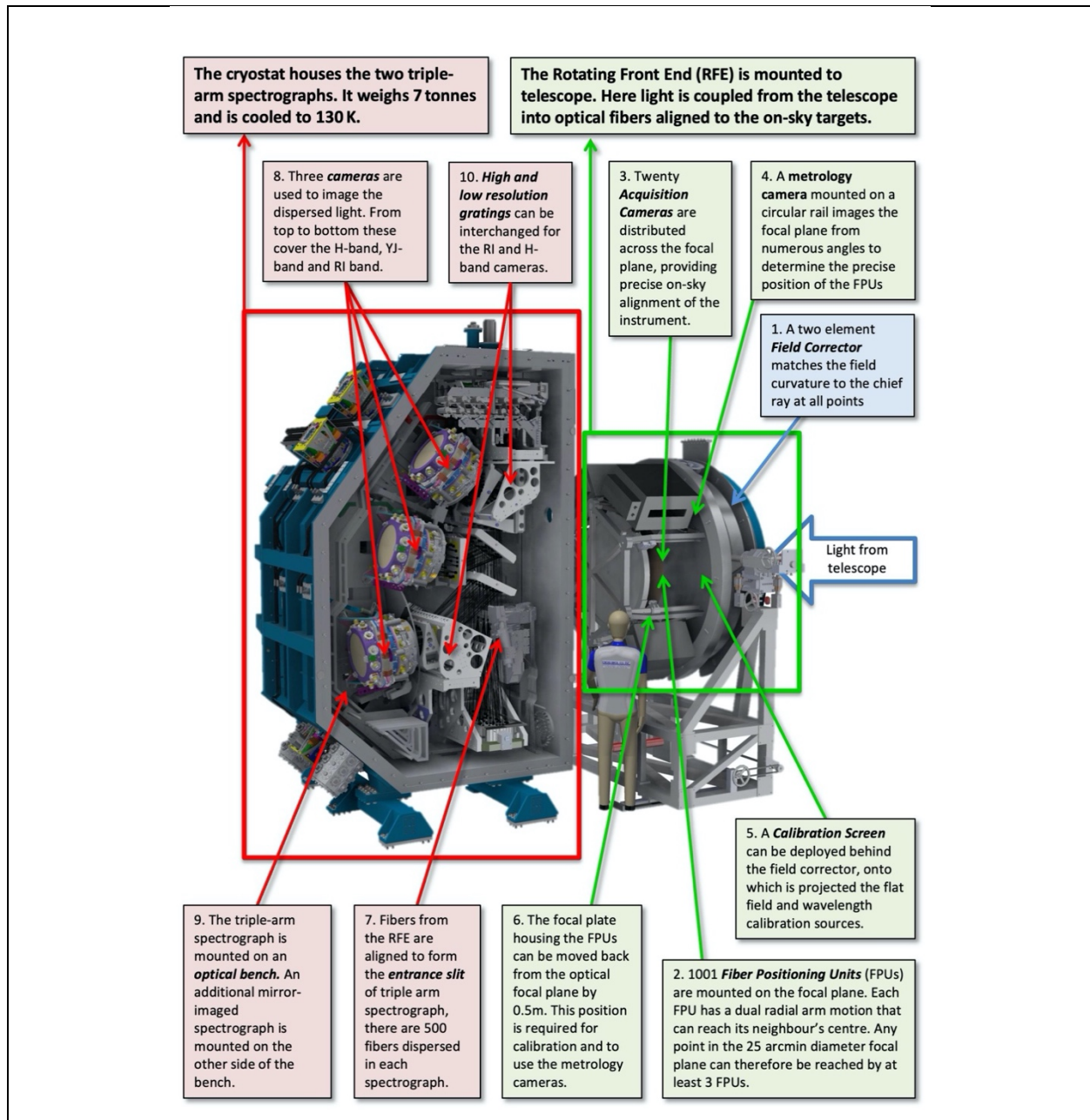


Figure 1. Overview of the main components of MOONS front-end and spectrograph

The MOONS RFE is mounted to the telescope and contains the focal plate and fibre positioning system used to align the optical fibres to their desired on-sky locations. Each 1.2" aperture fibre is positioned using independently controlled, dual-arm fibre positioning units (FPU's) with an on-sky repeatability better than 0.05".

The two arms in each FPU provide a patrol area that allows the fibre to reach the centre of all its neighbouring FPU's, but not its own centre, giving a 'doughnut-like' patrol field, which is indicated in Figure 2. Ultimately this allows full coverage of the field of view where targets can be reached by a minimum of two FPU's in high proximity (10") for optimal sky subtraction (see 2.4). This overlapping of the patrol fields for different FPU's means that careful path planning is required to ensure that the arms do not collide [2]. This planning is executed within the MOONS dedicated observing preparation software developed at INAF.

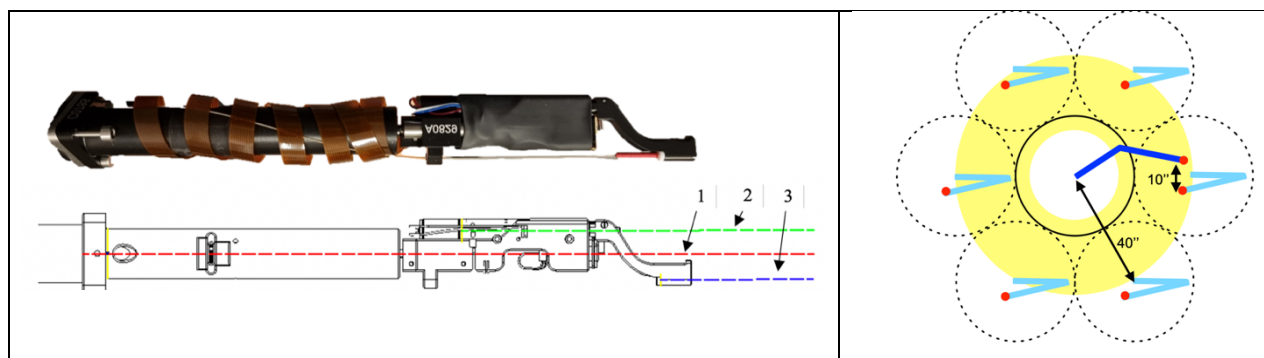


Figure 2. Left: MOONS FPU and diagram showing its alpha (1), beta (2), and optical (3) axes. Right: Footprint for a cluster of seven FPUs. The blue arms show the arms of the FPUs. For the central FPU the yellow doughnut indicates the area that the FPU can reach.

Twenty acquisition cameras (ACs) are distributed in the focal plane allowing excellent on-sky telescope alignment with the field using bright guiding stars that can also provide secondary guiding to ensure the fibres remain aligned to their targets during a long observation. The ACs will therefore correct for any flexure in the instrument and any misalignment in the rotation angle of the instrument. There are twenty cameras distributed across the plate radiating from the centre in a spiral pattern. Therefore, by rotating the field the ACs will sweep out the majority of the FOV of MOONS. This therefore enables the selection of a field rotation angle that maximizes both the number and the brightness of the acquisition stars that can be used.

The fibres then feed the light into the cryostat which houses two identical spectrographs, each handling 512 fibres. In each spectrograph the fibres are arranged in a curved entrance slit arrangement of 32 slitlets (16 fibres each). A collimator sits at the base of the optical bench in both spectrographs, reshaping the beam emitted from the optical fibres. The collimated beam is split into the three arms (*RI*, *YJ*, and *H*) by two dichroic beam-splitters. The *YJ* arm is equipped with a fixed transmission grating that disperses the light. The *RI* and *H* arms include interchangeable dispersive systems made by a combination of transmission gratings and prisms. The dispersed light in each channel is re-imaged onto a detector by an extremely compact and fast camera. The cameras consist of only 2 lenses and one mirror. The camera system achieves good image quality even with focal apertures faster than $F/1$ across most of the field. Figure 3 shows the optical design of each of the spectrographs for the high- and low-resolution configuration.

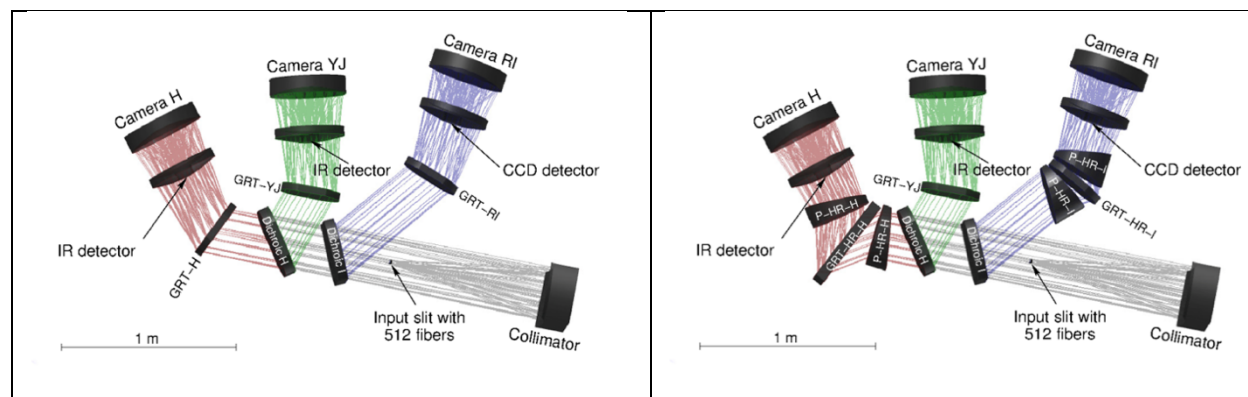


Figure 3. Optical design of the MOONS spectrographs in their low- (left) and high-resolution (right) configurations.

Each of the six cameras in MOONS uses a 4K x 4K array that is mounted in the camera lens. The two infra-red channels (*YJ* and *H*) will exploit the new Hawaii 4RGs 15 μ -pixel detectors and the visible channel (*RI*) will use fully depleted Lawrence Berkeley National Laboratory (LBNL) red-sensitive CCDs. In its low-resolution mode setup provides a complete wavelength coverage across 0.645 μ m – 1.8 μ m at R~4000-7500. In high-resolution, three windows are

observed simultaneously at $R \sim 9000$ in RI, $R \sim 4000$ in YJ, and $R \sim 19700$ in H. The exact wavelength regions covered by MOONS are listed in Table 1.

Table 1. Summary of MOONS main parameters

Parameter	Value
Telescope	VLT, 8 m
Field of view	25 arcminutes in diameter
Multiplex	1001
On-sky aperture of each fibre	1.2 arcseconds
Field coverage	> 3 fibres can reach any point in the focal plane
# of fibres within a 2-arcminute diameter	7
Minimum fibre separation	10 arcseconds
Spectral channels	<i>RI</i> , <i>YJ</i> and <i>H</i> bands observed simultaneously
Resolution modes	Low and high resolution
Low-res simultaneous spectral coverage	0.64 – 1.8 μm
Low-res spectral resolution	$R_{RI} = 4100$, $R_{YJ} = 4300$, $R_H = 6600$
High-res simultaneous spectral coverage	$\lambda_{RI} = 0.76 - 0.89 \mu\text{m}$, $\lambda_{YJ} = 0.93 - 1.35 \mu\text{m}$, $\lambda_H = 1.52 - 1.64 \mu\text{m}$
High-res spectral resolution	$R_{RI} = 9200$, $R_{YJ} = 4300$, $R_H = 19700$
Throughput	> 30% in low resolution, > 25% in high resolution
Sensitivity (point sources) in 1 hr integration	See Figure 3 for details
Continuum high res	S/N > 60 at $H_{AB} \sim 17$ and $RI_{AB} \sim 17.5$
Continuum low res	S/N > 5 at $\text{mag}(AB) \sim 23$ rebinning to $R = 1000$ after sky subtraction
Emission lines	S/N > 5 for a line flux of $> 2 \times 10^{-17} \text{ erg s}^{-1} \text{ cm}^{-2}$, FWHM = 200 km s^{-1}

2.2 MOONS Operational overview

2.3 Setup and acquisition

MOONS is versatile instrument that will allow astronomers to operate efficiently in both a survey run of large sky areas or in a single observation/experiment. To achieve this, MOONS design is optimised to keep instrument setup and acquisition time as short as possible by configuring its different mechanisms in parallel during the telescope *preset* (slewing to target field and start of guiding). In particular, the spectrograph mechanisms are very quickly set. These include the grating exchange mechanisms moving from one resolution grating to the other and the slit dither position. After the telescope has reached its final position and it is guiding, a small correction to the pointing (*X*, *Y*, and rotation) is done using the MOONS acquisition cameras. The images of all active acquisition cameras are taken and analysed by the software to automatically retrieve their centroids and calculate any necessary offsets to bring all targets as aligned as possible to the fibres. This procedure can continue in the background as a form of secondary guiding, by applying small corrections whenever necessary. This can be very useful in case of long observations.

The fibre positioners return to their default (initial) position at the start of any observation. This provides the possibility to continue immediately start the science exposure in the case that a new observation that has the same fibre configuration as the previous observation. This can occur for example when repeating an observing block.

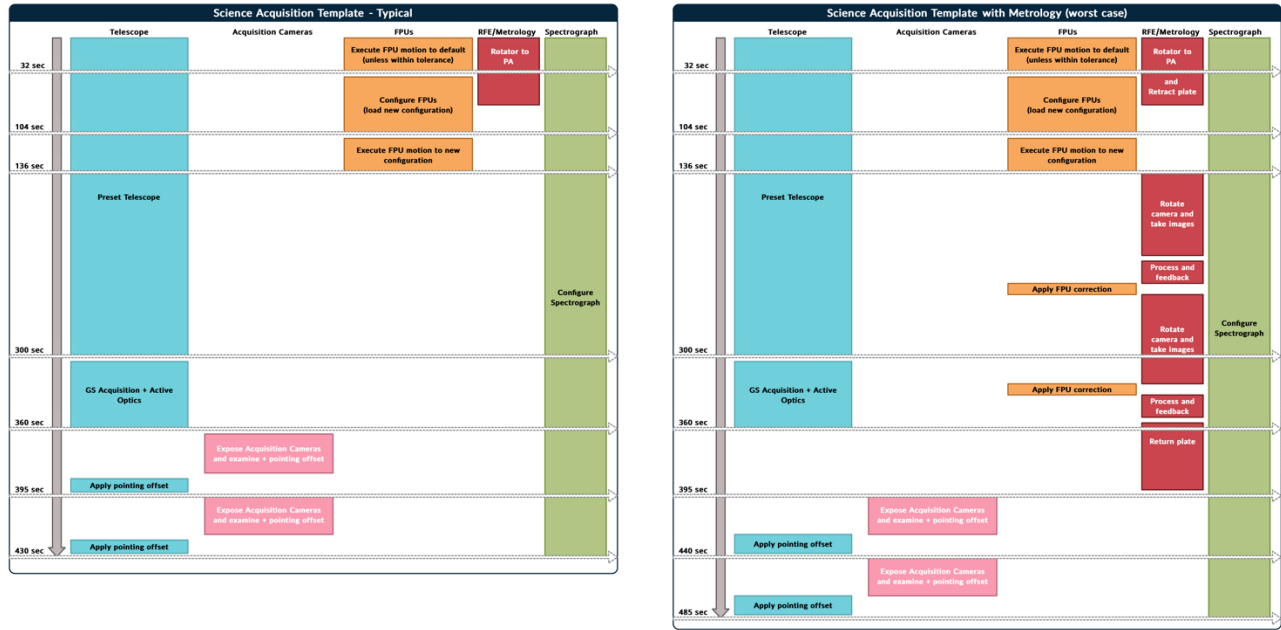


Figure 4. Operational breakdown of instrument actions during a MOONS acquisition procedure for the baseline (left) and for a non-standard observation that requires a metrology measurement correction (right).

The total FPU setup to their science position, including the return to default position, loading the new waveforms, and executing the movement to their final position takes ~ 2 min. For this reason, in a survey type of observation when the telescope slews are typically small, the total acquisition time will be dominated by guide star acquisition and acquisition camera adjustments, which should typically be done in a few minutes. This means that MOONS only needs ~ 2 min to start science exposures, when mapping a typical survey footprint, or up to ~ 7 -8 minutes when moving large telescope offsets in between observations.

2.4 Observing strategies

The main variation in a MOONS observation comes from the sky subtraction strategy selected by the astronomer. MOONS offers three observing strategies or modes to observe that are linked to a required sky subtraction accuracy requirement. Reaching the best sky subtraction comes at the expense of either more fibres used to monitor the sky or reduced total on-source observing time due to sky offsets. Therefore, to provide sufficient flexibility for the astronomer to optimize the strategy for their science, MOONS offers a Stare, StareNod, and X-switch observing strategy. These strategies are illustrated Figure 5. For each case, Figure 5 shows the distribution of the fibres in the slit.

Stare observations maximise the number of fibres allocated to targets, with a percentage of them (typically $\sim 10\%$) allocated to sky positions. This is the typical strategy used in visible wavelength MOS instruments. However, this observing strategy does not fully account for temporal and spatial variations of the sky at near-IR wavelengths. In addition, since the sky is not observed through the same optical path as each target fibre, the resulting line spread function of the science and target spectra can cause additional residuals. To mitigate for this, a mean sky is calculated using the sky fibres that are closest to each target fibre in the slit and, to a second order of priority, closest in sky coordinates. The number of fibres used to construct the sky spectrum associated to each target can be selected by the user. The best balance between the number of fibres used to construct each sky spectrum and the sky-target fibre separation (in the sky and the slit), will be found during instrument commissioning.

The StareNod strategy allows the user to map to include sky offsets during the observation where all the target fibres are positioned in blank sky locations. This allows the sky to be subtracted using a sky spectrum observed with the same fibre and thus identical line spread function. This removes the impact of the image quality variations across the detector that can create sky subtraction residuals in Stare, at the expense of on-source exposure time. Also, instead of using an

empirical sky model as in Stare, StareNod subtracts a single sky spectrum and thus the SNR of the resulting sky corrected spectrum is affected by twice the detector pixel noise and the sky spectrum photon noise.

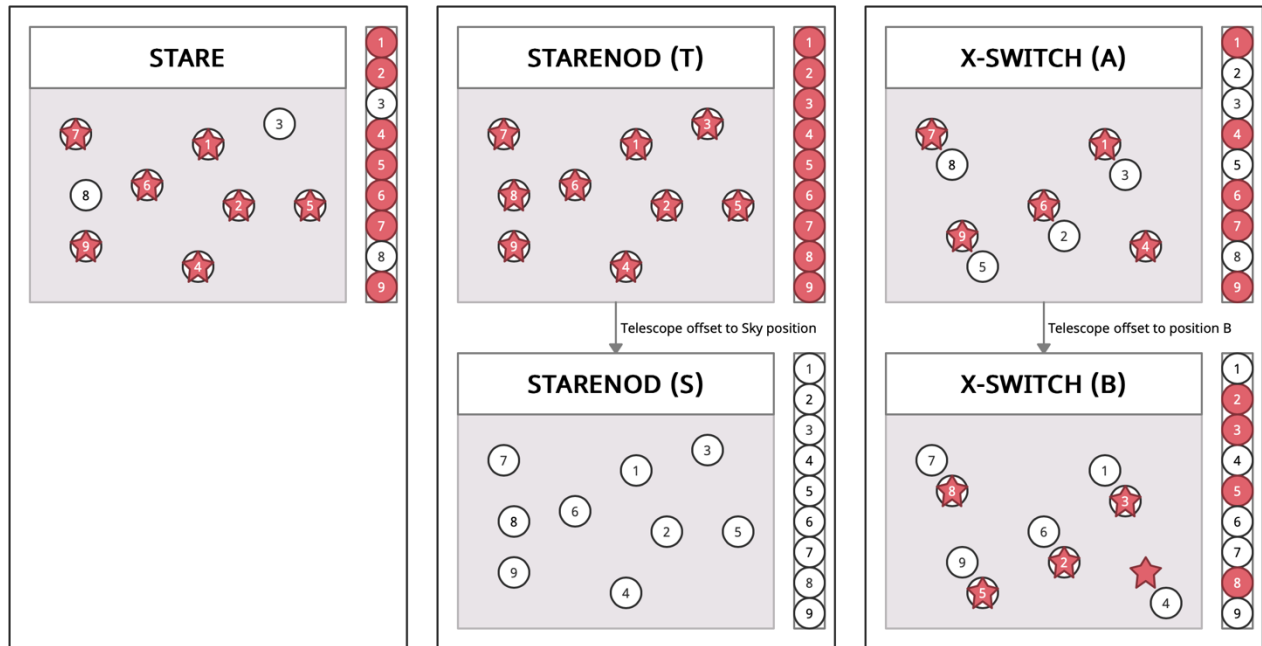


Figure 5. Diagram to illustrate MOONS observing strategies with fibres in targets and sky positions. In each case, an example of their distribution in the slit is also shown.

Finally, the X-switch strategy is designed to provide the best sky subtraction to the science spectra. In X-switch each target fibre is paired with a sky fibre as close together as possible (10-30 arcsec separation) so that a fibre is observing the sky simultaneously to account for temporal variations and at a small separation to account for spatial variations. Offsets between A and B positions are done in between each exposure to also have the sky observed through the same fibre as the target, to account for the image quality variations. This strategy although ideal to reach the faintest targets and remove undesired effects from sky subtraction, provides half the target fibres in each observation. In addition, when the 10 arcsec separation is used, the fibre allocation efficiency can be impacted and reach only ~70% due to conflicts arising from the close pairing of the FPU's. This of course depends on each case and on the number of available targets and their priorities in the field of view.

2.5 Observing preparation

The execution of a MOONS observation at the telescope is defined within an Observing Block (OB) which contains an Acquisition and Science templates. The acquisition template contains all the parameters needed to configure the telescope and instrument for the observation as described in 2.3. The Science Template contains all the exposure parameters including integration time and the relevant offsets depending on the observing strategy as described in 2.4. Critically, the acquisition template contains a pre-defined position of all the FPU's, where fibres are positioned in the respective targets (or sky) to be observed. This information is contained in an instrument *Parameter File* and a *Motor File* both of which are prepared by the astronomer and attached to the OB using the online ESO observing preparation tool (P2ui) that interfaces with the dedicated MOONS observing preparation software (MOONLIGHT) developed at INAF.

MOONLIGHT consists of an Optimisation procedure that performs the selection of targets from a user-defined input catalogue, accounting for the selected priorities and observing strategy, producing the final FPU configuration in the plate. This final position of fibres is checked to be conflict-free (thus avoiding FPU collisions) using a dedicated software named *Conflict Check*. This conflict-free configuration is saved in the *Parameter File*. The exact movements of

each positioner (i.e. the paths required to reach this final configuration) are produced by a dedicated path analysis software [2], which computes the motor steps required to safely drive each FPU from their default starting position to this final configuration. This is saved and passed to the instrument in the *Motor File*.

3. INSTRUMENT INTEGRATION UPDATE

3.1 Rotating front end

3.1.1 RFE structure

The RFE is the interface between MOONS and the VLT Nasmyth rotator. The structure contains a rotating unit that tracks the field during an observation, a retraction mechanism to switch the focal plate between a *science* and a *calibration* position, a calibration screen open/close mechanism, and an independent rotation mechanism holding the metrology camera system. The RFE contains the field corrector - which is the first optical element in MOONS - the focal plate with all 1000 fibre positioners and 20 acquisition cameras, and the calibration unit.

The RFE structure assembly has been completed at the IfA in Lisbon [7]. All the mechanisms have been verified and the system is ready for integration into the instrument at UKATC in Edinburgh.

3.1.2 Field corrector

To obtain excellent image quality across the full FOV of the VLT a large Field Corrector lens is used. This ~900 mm diameter window forms the first optical component in the MOONS instrument. Two lenses and mounting structure compose this optical interface that correct the off-axis aberrations of the telescope, as well as determining the shape of the focal surface and the pupil location.

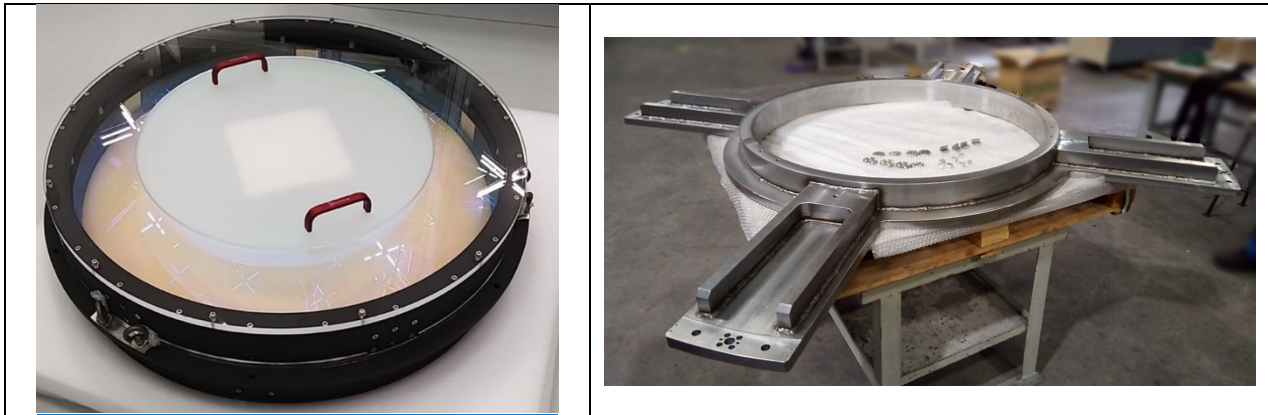


Figure 6. Field corrector assembly and structure

The MOONS field corrector structure was finished and fully verified with metrology. The field corrector assembly is now ready for shipment and commissioning in Paranal. This will happen in advance of the arrival of the rest of the MOONS instrument. Further details can be found in [7].

3.1.3 Fibre positioning system

All the MOONS FPUs have now been manufactured by MPS microsystems and delivered to UKATC. A verification and calibration procedure is carried at the UKATC lab on each of the FPUs before they are installed in the plate. As of late June 2022, 659 FPUs are already fully verified, calibrated, and installed in the MOONS focal plate. Details can be found in [6].

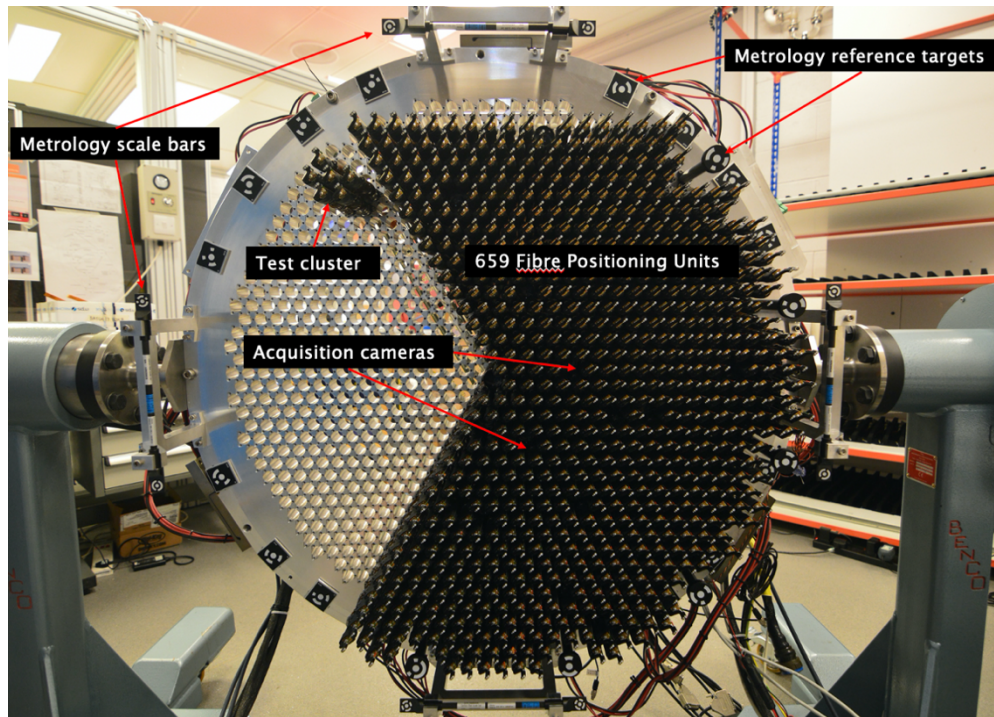


Figure 7. MOONS focal plate during ongoing installation of FPU. The plate also has partial integration of Acquisition Cameras and metrology targets/scale-bars.

3.1.4 Retraction mechanism

The focal plane of the VLT lies just behind the field corrector lens, which makes inspection of the fibre positions and/or calibrating the fibres extremely difficult. The entire plate on which the FPU are mounted can therefore be retracted by ~500 mm from the focal plane of the telescope to allow better access to the space between the fibres and the field corrector lens. The retracted plate position is used for the calibration of the instrument by the metrology system and the calibration unit. The technical details of the mechanism can be found in [7].

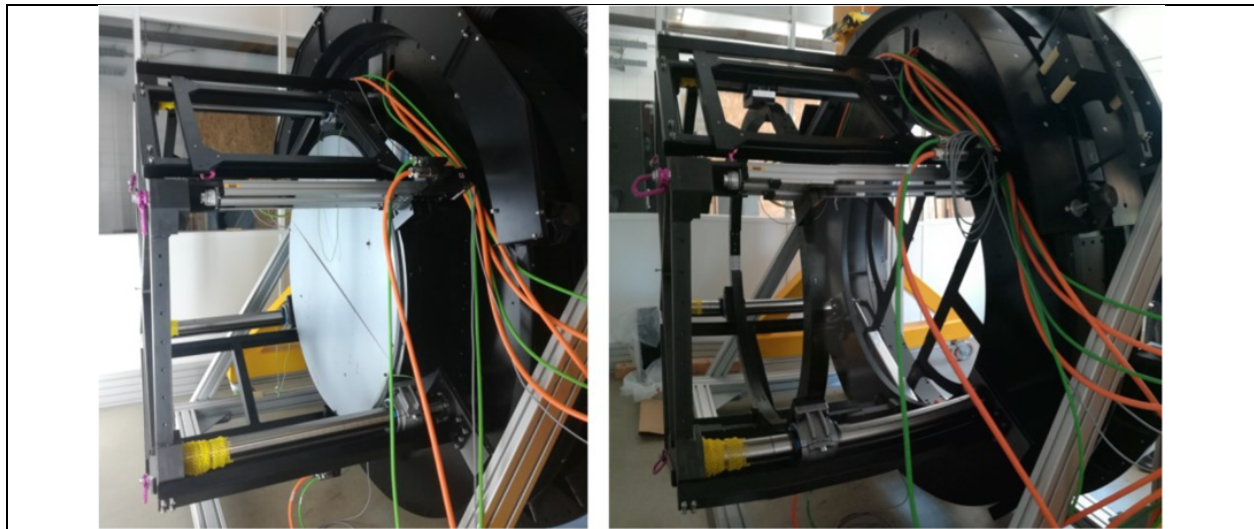


Figure 8. MOONS RFE structure with the retraction mechanism in science position (left) and calibration position (right).

The retraction mechanism is now installed and operational in the RFE. Figure 8 shows two images of the retraction mechanism placing the focal plate position in *science* and in *calibration* positions. The *calibration* position allows the fibres to see the closed calibration screen and illuminated by the calibration unit lamps. Similarly, the *calibration* position allows the metrology camera to see the complete FOV during its rotation to produce a calibration measurement. The mechanism has been verified with a repeatability of <15 micron and a retraction time from *science* to *calibration* position of 30 seconds.

3.1.5 Metrology system

A single camera installed in a rotating mechanism in the rotating front end can obtain a number of images of the focal plane from a set of angles around a full 360-degree rotation. The images are analysed with dedicated photogrammetry software to recover the accurate positions of the FPU fibres at any given time. The metrology camera can measure position to an accuracy of 10-15 microns. Due to the location of the focal plane within MOONS it is necessary to move to the plate to the *calibration* position (see 3.1.4) before the metrology measurements can be taken. The metrology system requires fixed reference targets and scale bars distributed across the plate that provide calibrated reference points for determining the real-world pixel scale of the cameras.

The metrology system has been fully tested in a partially populated MOONS focal plate with a fibre detection effectiveness of 100%. Figure 9 shows an example test in which the 3D positions of the metrology targets in the FPU beta arms are recovered. These are then processed by a dedicated identification algorithm that retrieves the fibre position, orientation of the beta arm, and association to each FPU. This information is then passed to the FPU control software to update the current configuration information and, in the case of a failure, return the system to its default position.

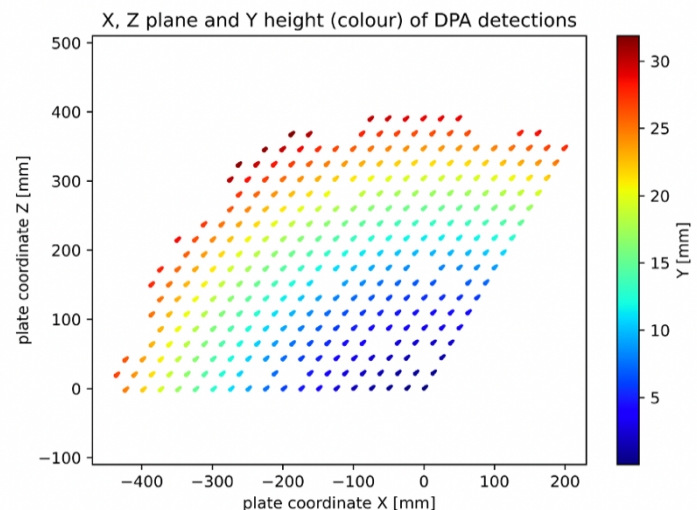
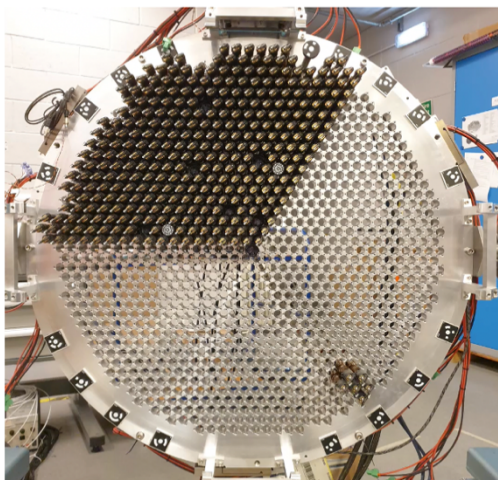


Figure 9. Example of a metrology measurement in a partially populated plate during FPU integration

The metrology camera rotation mechanism in the RFE has been tested in Lisbon together with its dedicated illumination system of 6 LEDs. The system was shown to be able to map and recover the plate coordinate system with the required accuracy. The final integration of the metrology system is done once the focal plate is installed in the RFE and the end-to-end system can be fully verified. Further details on the MOONS metrology system can be found in [8].

3.1.6 Acquisition cameras

Coarse acquisition of a MOONS field will be achieved using the VLT Guide Probe. Fine acquisition will be obtained using the Acquisition Cameras (ACs) to observe bright stars distributed across the MOONS FOV. The ACs will correct for any flexure in the instrument and any misalignment in the rotation angle of the instrument. Each AC occupies the footprint of one FPU and will have an on-sky FOV of 0.353 square arcmin. The twenty cameras are distributed radially

to give good coverage of the instrument focal plane, but only a small number of cameras (>3) will be used in a typical observation.

At time of writing, there are 14 of 20 cameras integrated into the FPU plate. The cameras must be integrated in sequence along with its neighbouring fibre positioning units. Figure 10 shows one of the cameras integrated in line with the most recent line of positioners, as well as a view of a fully embedded camera.



Figure 10. Acquisition cameras installed in the MOONS focal plane around the FPUs.

Testing has shown that there is no interference between the camera barrels and adjacent FPUs, a necessary check given the proximity of moving parts to the cameras. The single control cable from each of the cameras runs across the back plane of the FPU plate to the control boxes mounted around the outer ring. From there the power and control cables are routed via the retraction mechanism to a control cabinet on the outer ring of the RFE.

On telescope testing of a camera is scheduled to take place in late 2022 during the installation of the Field Corrector on the VLT.

3.1.7 Calibration Unit

The MOONS instrument contains a calibration unit [4] that will illuminate all the fibres at the same time. This is done by retracting the focal plate and closing a screen behind the field corrector. The closed screen is then illuminated by an off-axis source. The wavelength calibration is achieved by projecting the flux from a Thorium-Argon source onto the same screen.

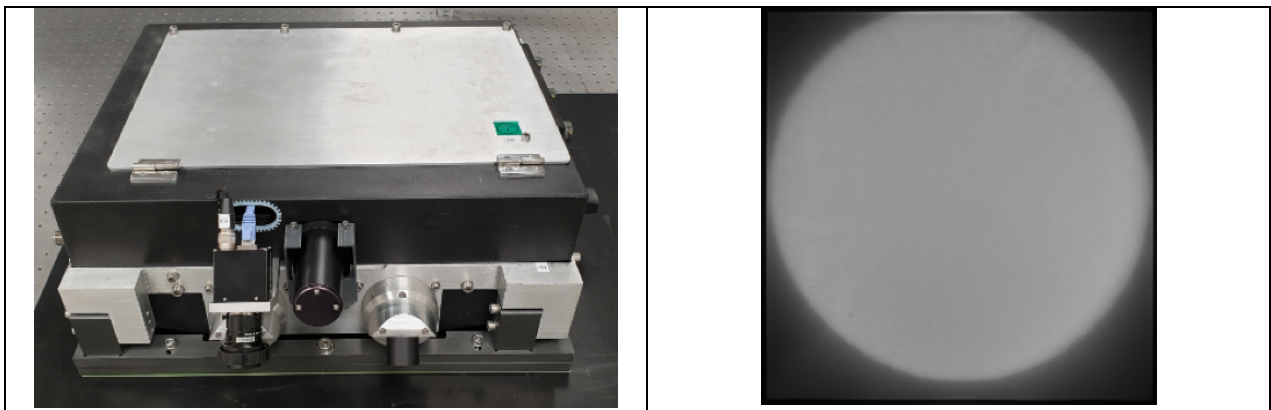


Figure 11. MOONS calibration unit (left) and image of the illuminated calibration screen (right)

The calibration unit is now completed, and it is ready for installation in the RFE. Figure 11 shows the fully assembled calibration unit before integration to the RFE. The flat field illumination has been fully tested and shown to be spatially flat to around 1% across the full screen (Figure 11). This is achieved using a digital micro-mirror array device to compensate for any non-uniformity in the projected image. The achieved performance guarantees the capability to calibrate the fibre-to-fibre transmission for optimal sky subtraction.

3.2 Spectrograph

Side 1 of the spectrograph is now fully populated and testing is ongoing. Previous cooldowns confirmed that camera alignment/image quality, wavelength coverage, and resolving power are achieved on YJ and RI band. H band testing is ongoing. An updated description of the spectrograph integration and testing results can be found in [9].

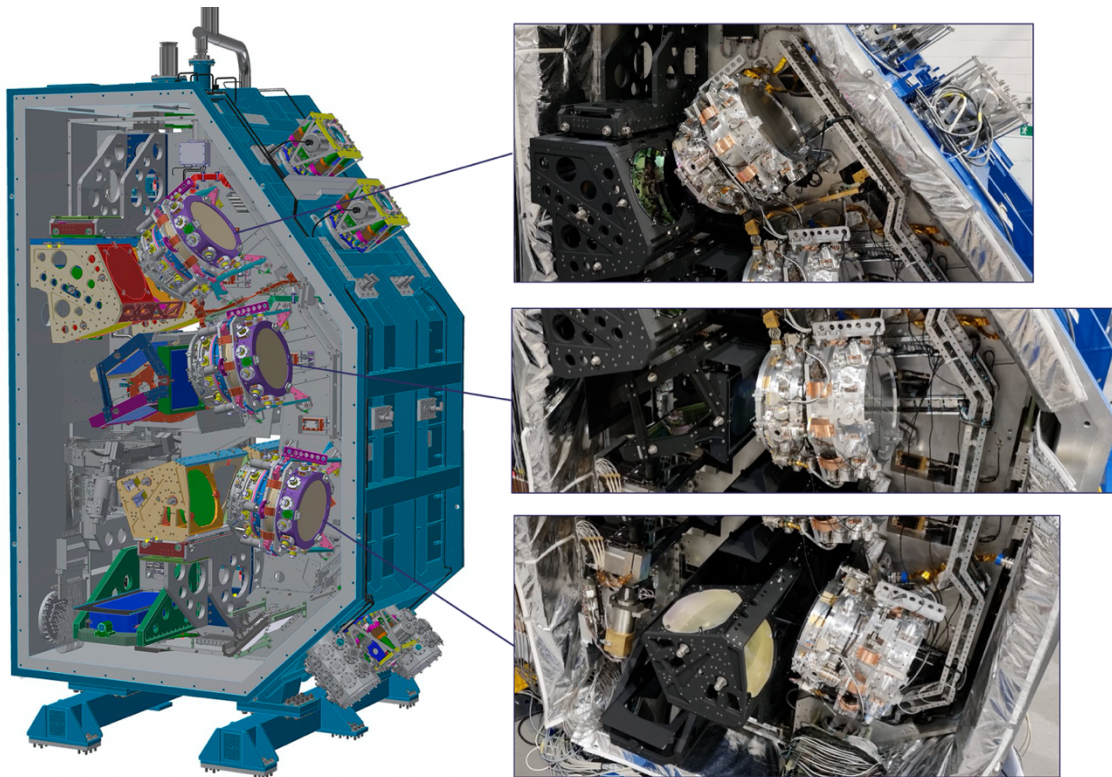


Figure 12. Three channels of MOONS, H, YJ, and RI from top to bottom, in the fully populated side 1 of the spectrograph.

3.2.1 Cameras

There are three pairs of cameras in MOONS; two RI band, two YJ band and two H band cameras. The design of the cameras is nearly identical. All the optical elements, the mirrors and the L1/L2 lens assembly (glued together) have been completed and delivered by Winlight. Each camera contains a detector adjustment module, consisting of motor driven stages that allow the detector to be moved in 3-axes to ensure the optimum focus.

The alignment of all the cameras has been completed in Cambridge and three of them have been fitted and tested in side 1 of the spectrograph (see Figure 12). The alignment performed in Cambridge [10] was confirmed to be correct by the image quality tests performed during the latest instrument cooldowns [9]. The remaining cameras will be installed for the next cooldown together with all the optics of side 2.

3.2.2 Slit assembly

The assembly of the slit and the corresponding mechanisms can be seen in Figure 13. Each of the two slits is comprised of 32 slitlets, each slitlet containing 16 fibres. The relative alignment of the slitlets has had to meet two very tight requirements: to ensure throughput is maintained for all fibres, there has only been a 3mrad tilt allowed on each slitlet, while the slitlets must have a mechanical offset of <5 microns. Both these properties were demonstrated in GEPI before shipment to Edinburgh and have been verified in the cold instrument at the UKATC. The second assembled slit is nearly complete and will be shipped to the UKATC for installation later in the year

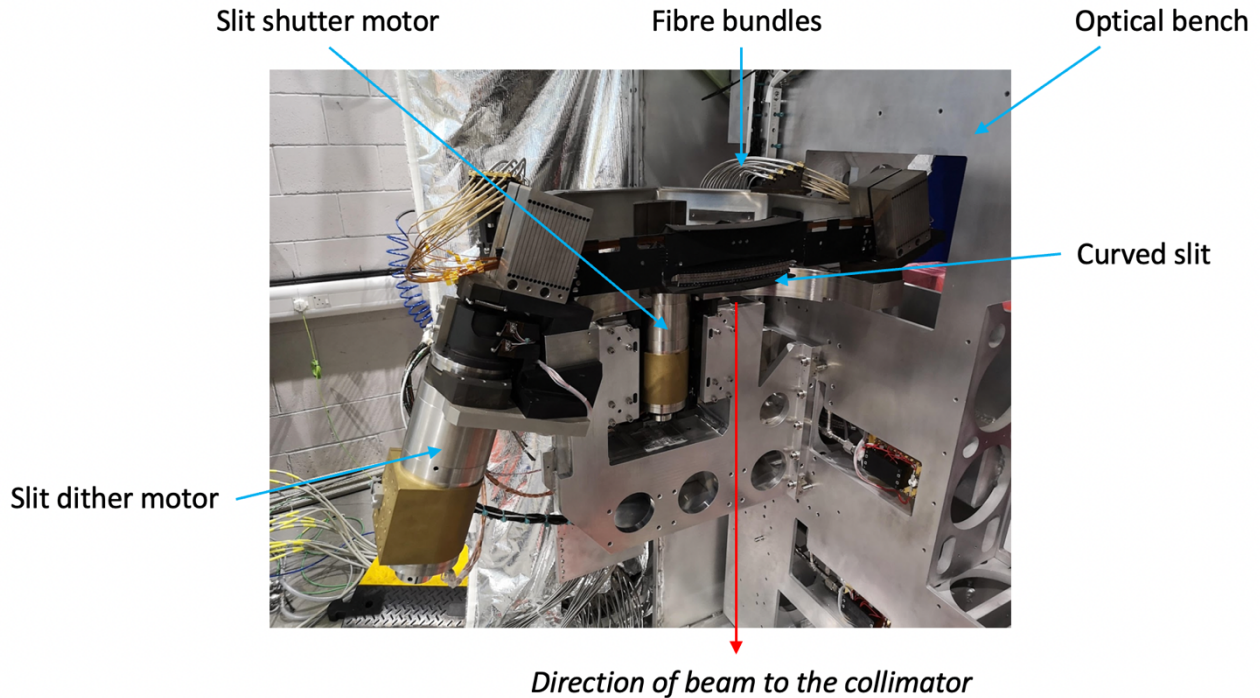


Figure 13. Slit assembly, showing the slit and the associated mechanisms

Figure 14 shows a small section of the detector, containing imaged emission lines from a test source in the lab (see [9] for details of these and more spectrograph tests). While also illustrating a great deal about the image quality achieved in the early cooldowns, this image is primarily to show the groupings of the fibres in the slitlets. In a perfect spectrograph all the spots would be in a perfectly aligned horizontal position, but small jumps are visible between the groups of 16 fibres in each slitlet. These jumps are effectively removed during calibration and it has already been demonstrated that they are within the acceptable limits for the MOONS data reduction software.

3.2.3 Slit dither mechanism

To avoid any defective areas of the detectors and to mitigate the impact of persistence, it will be possible to offset the slit by a fixed amount so that the flux from the fibres illuminates a different region of the detectors. The exact offset will be equivalent to 4 pixels on the detector. Spectra on the detector are separated by ~8 rows of pixels, so an offset of 4 rows will place the spectra in a region of the detector not illuminated in the previous observation. This allows the effects of bad pixels and persistence to be minimized.

The slit dither mechanism has been verified within the assembled instrument. It has been shown that a full 13 pixels of vertical movement on the detector can be achieved, which allows some adjustment of where the exact operating positions are. Early testing has also demonstrated that the mechanism is highly repeatable over multiple motions for short timescales, further testing will be made on long term stability.

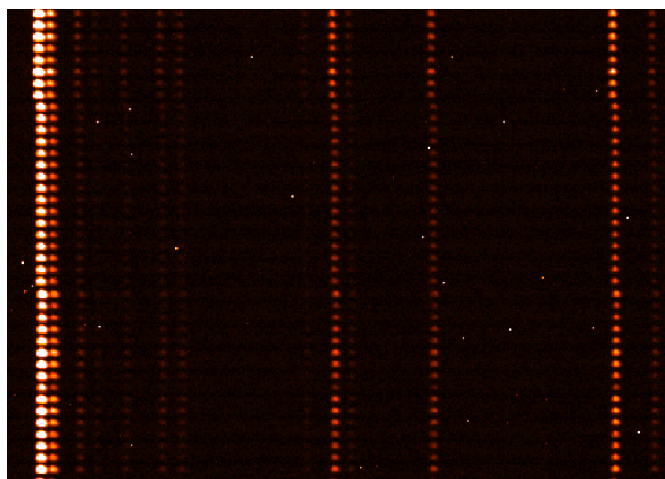


Figure 14. Arc line features imaged on the detector

3.2.4 Shutters

Two shutters are used with in the spectrograph: the *Slit Shutter*, which fully blocks light emitted from any of the fibres into the spectrograph making the system completely light tight, and the *RI-band Shutter*, which is placed immediately prior to the RI-band camera, thus allowing this channel to be closed independently of the IR-channels.

The slit shutter is complete and has been tested cold within the instrument, showing that it meets many of the basic requirements.

To ensure uniform exposure times on both the RI cameras, a single RI-band shutter is used to vignette the beams in both channels at once. This has resulted in a very large cryogenic component, which has challenging limits on the required acceleration, allowed deformation (due to mechanical proximity to the RI cameras), and on mass. Consequently, the component has gone through a number of design iterations. The final design utilises a large single-piece shutter that is nearly 2 metres in diameter. This is currently being manufactured, and once complete it will undergo vibration testing, before black coating and installation in the instrument.

3.2.5 Detectors

Most of the cold testing has been carried out with only engineering devices for the YJ and RI channels. Despite their slightly lower performance, it has been possible to demonstrate several key elements of the detector design. For instant, the tight tolerances on detector rotation and mask alignment have been achieved.

In each of the MOONS cameras the detector sits in the centre of the optical beam, with communication and thermal control delivered through the spider legs of the detector box. To minimise the vignetting caused by the structure, the detector preamps have been packed into a small volume immediately behind the detector, which is especially difficult for the 64 channels of the MOONS infrared devices. The cold testing so far, has therefore been used to demonstrate that the cross talk between channels is acceptable. Likewise, with multiple NGCs running simultaneously it has also been possible to show that there is no electrical noise induced between detectors.

For the infrared devices there is a noticeable glow caused by the read-out electronics, which effects the lower portion of the detector. Although stable, this marginally increases the readout noise for some of the device. Testing has shown that the glow can be removed completely by running the detectors in an unbuffered mode, but this leads to greater cross talk between the channels of the detector. It has been decided to keep the devices in the original buffered mode, and accept the slightly increased noise. A compromise of using fewer up-the-ramp readouts and a change to the readout resistors

minimises the impact of the problem: it will ultimately lead to only a few additional electrons of read noise, across the bottom portion of the device.

MOONS is utilising LBNL deep depleted CCDs for the RI channels as they have excellent quantum efficiency right out to 0.9 μm . They have not been used on a VLT instrument before, so the successful demonstration of the engineering grade in the instrument is also a good milestone.

The first science grade engineering device has now been installed for the H-band. As is expected, this has better cosmetic quality across the whole device and will allow full verification of the detector noise performance and the instrument's dark levels.

3.3 Control Software

The Control Software of MOONS is based on the standard of the VLTSW standard, in which the Instrument Control Software (ICS) is responsible for the direct control of all hardware devices. By means of Observation Software (OS) the exposure sequence of an observation as well as the interactions between the different subsystems are coordinated at a higher level. The latter also communicates with the Telescope Control Software (TCS). The Maintenance Software (MS) package eventually is used for instrument configuration and technical calibrations. Hierarchically, MOONS is divided into two main systems, MOONS1 for the spectrograph, while MOONS2 is assigned to control the RFE. On top of that, a Supervisory OS (SOS) will coordinate both systems.

In terms of software development, for MOONS1, most of the configuration and development of the device drivers at the ICS level are ready and are being verified once the hardware is available in the integration center of the UKATC. Values of the sensors in the cryostat have been monitored for several months. Although, the scientific detectors are being tested in a standalone mode, and soon will be integrated with the OS. Parallely, in MOONS2, effort has been spent in the path analysis, fibre positioner and metrology camera software can control an array of fibre positioners without significant risk of collision. The software has been tested with a cluster of 12 positioners on the focal plate. The acquisition cameras are able to take exposures and analysing acquisition images, and high-level panels were created to display a mosaic of images captured by the 20 acquisition cameras. The calibration system truth camera can make exposures and analysing flat-field images, while the calibration projector software implementation is underway. At SOS level, the implementation of the scientific templates has been started, and should drive the effort in the second semester of this year.

4. DELIVERY

The MOONS project is now in the final phase of the assembly and verification. Testing of the spectrograph alignment has been successfully completed for 3 of the 6 MOONS channels [9] confirming compliance of key requirements such as image quality, transmission, and resolving power. All the major sub-systems in the front-end have been assembled and the serial production of the 1000 fibres and the fibres positioners is now completed. The plate population has completed two of the three sectors and will be integrated into the RFE later in 2022. The delivery of the instrument is currently planned for 2023 and start science operations in 2024.

5. ACKNOWLEDGMENTS

The Portuguese team was supported by Fundação para a Ciência e a Tecnologia (FCT, Portugal) through the research grants UID/FIS/04434/2019, UIDB/04434/2020 and UIDP/04434/2020. The Fully depleted CCDs used in MOONS were developed at the Lawrence Berkeley National Laboratory. The CCD development work was supported in part by the Director, Office of Science, of the U.S. Department of Energy under contract No. DE-AC02-05CH11231.

6. REFERENCES

- [1] Michele Cirasuolo, et al., "Crescent MOONS: an update on the ongoing construction of the new VLT's multi-object spectrograph," Proc. SPIE 11447, Ground-based and Airborne Instrumentation for Astronomy VIII, 1144717 (2020)
- [2] Steven M. Beard, et al., "MOONS Fibre Positioner Control and Path Planning Software", Paper 12189-35 SPIE Astronomical Telescopes + Instrumentation (2022).
- [3] Isabelle Guinouard, et al., "MOONS - Multi Object Spectroscopy for the VLT: Final performances and integration of the fibres", Paper 12188-212 SPIE Astronomical Telescopes + Instrumentation (2022).
- [4] David Lee, et al., "MOONS – multi-object spectroscopy for the VLT: DMD based instrument calibration system ", Paper 12188-182 SPIE Astronomical Telescopes + Instrumentation (2022).
- [5] Oscar Gonzalez, et al., "MOONS – Multi Object spectroscopy for the VLT: overview and instrument integration update ", Paper 12184-38 SPIE Astronomical Telescopes + Instrumentation (2022).
- [6] Stephen Watson, et al., "MOONS fibre positioning module: instrument build overview", Paper 12188-79 SPIE Astronomical Telescopes + Instrumentation (2022).
- [7] Alexandre Cabral, et al., "MOONS – Multi Object spectroscopy for the VLT: integration and tests of the Field Corrector and the Rotating Front End", Paper 12184-251 SPIE Astronomical Telescopes + Instrumentation (2022).
- [8] Oscar Gonzalez, et al., "MOONS – Multi Object spectroscopy for the VLT: Design and testing of the MOONS metrology system", Paper 12188-138 SPIE Astronomical Telescopes + Instrumentation (2022).
- [9] Martin Black, et al., "MOONS – Multi Object spectroscopy for the VLT: Spectrograph Performance", Paper 12184-273 SPIE Astronomical Telescopes + Instrumentation (2022).
- [10] Martin Fisher, et al., "Optical performance and results from the alignment and testing of the cameras for the MOONS spectrograph", Paper 12184-258 SPIE Astronomical Telescopes + Instrumentation (2022).